

Lattice Boltzmann simulation of EGM and solid particle trajectory due to conjugate natural convection

J. Alinejad^{1,*}, J. A. Esfahani²

¹Department of Mechanical Engineering, Sari Branch, Islamic Azad University, Sari, I. R. Iran

²Department of Mechanical Engineering, Ferdowsi University of Mashhad, Mashhad 91775-1111, I. R. Iran

Received 1 March 2015;

revised 9 November 2015;

accepted 21 November 2015;

available online 5 January 2016

ABSTRACT: The purpose of this paper is to investigate the EGM method and the behavior of a solid particle suspended in a two-dimensional rectangular cavity due to conjugate natural convection. A thermal lattice Boltzmann BGK model is implemented to simulate the two dimensional natural convection and the particle phase was modeled using the Lagrangian–Lagrangian approach where the solid particles are treated as points moving in the computational domain as a result of the fluid motion. Entropy generation due to heat transfer irreversibility, isotherms, streamlines and Nusselt numbers were obtained and discussed. Total entropy generations in various cases are also reported and optimum case is presented based on minimum entropy generation.

KEYWORDS: conjugate convection; entropy generation; lattice Boltzmann model; Lagrangian–Lagrangian (L–L); particle trajectory

INTRODUCTION

The objective of this study is to develop a Lagrangian-Lagrangian based numerical scheme to simulate the behavior of solid particle in a rectangular cavity due to conjugate natural convection. The problem of natural convection in an enclosure has been a widespread topic of research, due to its occurrence in industrial and technological applications, such as electronic cooling [1,2], cooling of the nuclear or chemical reactors [3,4] and the heat and mass transfer processes in cryogenic fuel and vertical storage tanks [5–11].

In these works, the regimes of convective heat transfer in closed vertical volumes were analyzed in detail for the conditions when the thermal fluxes supplied to the liquid are uniformly distributed in the base zone and over the bottom and lateral surfaces. The spatial and temporal structure of convection at a sine distribution of the thermal flux on the lateral wall of the vertical cylinder was presented in [12]. The conjugate problem of natural convection in a vertical tank partially filled with the liquid was analyzed in [13] under the conditions of the supply of a uniform heat flux to the external side of the lateral wall and a simultaneous heat removal through the local sinks located in the tank lateral wall. The mathematical modeling of unsteady regimes of natural convection in a closed cylindrical region with a heat-conducting shell of finite thickness was carried out in [14]. Numerous studies of various physical systems based on EGM are reported in literature [15–19].

Abolfazli and Alinejad [15] analyze the entropy generation due to conjugate natural convection in an enclosure. Baytas [16] presented a comprehensive analysis on influence of Rayleigh number, Bejan number and inclination angle on entropy generation for natural convection in an inclined porous cavity. Transition criteria for entropy reduction of convective heat transfer from micropatterned surfaces were reported by Naterer [17]. Entropy generation in microchannel flow with presence of nanosized phase change particles was investigated by Alqaity et al. [18]. Vosoogh et al. [19] studied the effect of nanofluid on entropy generation and pumping power in coiled tube. Recently Lattice Boltzmann Method (LBM) has been developed as a new tool for simulating the fluid flow, heat transfer and other complicated physical phenomena. Compared with the traditional computational fluid dynamics methods, the Lattice Boltzmann is a mesoscopic approach based on the kinetic theory. It has many advantages, such as simple coding, easy implementation of boundary conditions, fully parallelism and there is no explicit requirement of fluid pressure calculation [20]. At present the applications of LBM have achieved great success in multi phase flow, chemical reaction flow, flow in porous medium, thermal hydrodynamics, suspension particle flow and magneto hydrodynamics. Chatterjee and Amiroudine [21] proved the multiscale mesoscopic lattice Boltzmann methods to be an efficient and inexpensive tool to simulate complex thermofluidic phenomena. Guo and Zhao [22] conducted the simulation for incompressible flow in porous media by using LBM. D’Orazio et al. [23] and Shu et al. [24]

*Corresponding Author Email: Alinejad_javad@iausari.ac.ir
Tel.: +989121083680

Nomenclature		
Be	Bejan number	u, v Velocities, m/s
g	Gravitational acceleration, m/s ²	x, y Coordinates, m
n	Normal direction on a plane	Greek Symbols
S_h	Entropy generation due to heat transfer	α Thermal diffusivity, m ² s ⁻¹
S_f	Entropy generation due to fluid friction	μ Dynamic viscosity, kg(ms) ⁻¹
N_s	Dimensionless total entropy generation	θ Dimensionless temperature
Nu_l	Local Nusselt number	Subscripts
Nu_m	Mean Nusselt number	c cold
Pr	Prandtl number	f fluid
Ra	Rayleigh number	h hot
T	Temperature, K	s solid

performed the numerical calculations for the natural convection in a cavity.

The scopes of this study are as follows:

- i) Implementing Lattice Boltzmann Method to simulate flow and thermal fields
- ii) Evaluate the simulations using Rayleigh Number ranging from 10^3 to 10^6 and compare the obtained results
- iii) Evaluate the simulations using different thermal solid resistances
- iv) Applying the Second Newton Law to trace the position of the solid particle in cavity flow

1) Lattice Boltzmann method

The lattice kinetic theory and especially the lattice Boltzmann method have been developed as significantly successful alternative numerical approaches for the solution of a wide class of problems [25–27]. The LBM is derived from lattice gas methods and can be regarded as a first order explicit discretization of the Boltzmann equation in phase space. This method (LBM) is a powerful numerical technique, based on kinetic theory, for simulating fluid flow [29] and heat transfer [30, 31], and has many advantages in comparison with conventional CFD methods mentioned previously. In contrast with the classical macroscopic Navier–Stokes (NS) approach, the lattice Boltzmann method uses a mesoscopic simulation model to simulate fluid flow [30].

It uses modeling of the movement of fluid particles to capture macroscopic fluid quantities, such as velocity and pressure. In this approach, the fluid domain is made discrete in uniform Cartesian cells, each one of which holds a fixed number of Distribution Functions (DF) that represent the number of fluid particles moving in these discrete directions. Hence depending on the dimension and number of velocity directions, there are different models that can be used. The present study examined two-dimensional (2-D) flow by a 2-D square lattice with nine velocities (D2Q9 model).

The velocity vectors $c_0 \dots c_8$, of the D2Q9 model are shown in Figure 1 For each velocity vector, a particle DF is stored. The velocities of the D2Q9 model are:

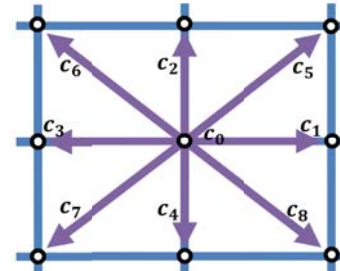


Fig. 1. 2-D 9-velocity lattice (D2Q9) model

$$c_k = \begin{cases} (0,0) & k = 0 \\ (\pm 1,0)c, (0, \pm 1)c & k = 1,2,3,4 \\ (\pm 1, \pm 1)c & k = 5,6,7,8 \end{cases}$$

where $c = \Delta x / \Delta t$ and k is the Lattice velocity direction.

The LB model used in the present work is the same as that employed in [30].

The DFs are calculated by solving the Lattice Boltzmann Equation (LBE), which is a special discretization of the kinetic Boltzmann equation. After introducing Bhatnagar–Gross–Krook (BGK) approximation, the Boltzmann equation can be formulated as below [26]:

$$f_k(x + c_k \Delta t, t + \Delta t) = f_k(x, t) + \frac{\Delta t}{\tau} [f_k^{eq}(x, t) - f_k(x, t)] + \Delta t c_k F_k \quad (1)$$

where Δt , c_k , τ , f_k^{eq} is the equilibrium DF, and F_k denote the lattice time step, the discrete lattice velocity in direction k , the lattice relaxation time, the equilibrium DF, and the external force in the direction of the lattice velocity, respectively. In order to incorporate buoyancy force in the model, the force term in equation 1 needs to be calculated in a vertical direction (y) as follows:

$$F = 3w_k g_y \beta \quad (2)$$

$$\theta = \frac{T - T_c}{T_h - T_c} \quad (3)$$

For natural convection, the Boussinesq approximation is applied, and radiation heat transfer is negligible. To ensure that the code works in the near incompressible regime, the characteristic velocity of the flow, $V_{natural} = \sqrt{\beta g_y \Delta T H}$, for a natural convection regime must be small compared with the fluid speed of sound.

Equilibrium DFs are calculated as:

$$f_k^{eq} = \omega_k \rho \left[1 + \frac{c_k \cdot u}{c_s^2} + \frac{1}{2} \frac{(c_k \cdot u)^2}{c_s^4} - \frac{1}{2} \frac{u^2}{c_s^2} \right] \quad (4)$$

where the weights of ω_k are $\omega_k = 4/9$ for $k = 0$, $\omega_k = 1/9$ for $k = 1, 2, 3, 4$ and $\omega_k = 1/36$ for $k = 5, 6, 7, 8$; and $c_s = c_k/\sqrt{3}$ is the lattice speed of sound. The macroscopic fluid variable densities and velocities are computed as the first two moments of the distribution functions for each cell:

$$\rho = \sum_{k=0}^8 f_k, \quad u = \frac{1}{\rho} \sum_{k=0}^8 f_k c_k \quad (5)$$

This model is explained in more detail in [32]. For the temperature field the g distribution is as below:

$$g_k(x + c_k \Delta t, t + \Delta t) = g_k(x, t) + \frac{\Delta t}{\tau_g} [g_k^{eq}(x, t) - g_k(x, t)] \quad (6)$$

The corresponding equilibrium DFs for fluid and solid, respectively, are defined as follows [30]:

$$g_k^{eq} = \omega_k T \left[1 + \frac{c_k \cdot u}{c_s^2} \right] \quad (7)$$

$$g_k^{eq} = \omega_k T \quad (8)$$

The temperature field is computed as:

$$T = \sum g_k \quad (9)$$

Evaluation of Nusselt number and thermal resistance:

Heat transfer between hot and cold walls was computed by local and mean Nusselt number which is given as

$$Nu_l = \frac{-1}{\theta_m} \frac{\partial \theta}{\partial n} \Big|_{wall} \quad (10)$$

$$Nu_m = \frac{1}{x} \int_0^x Nu_l dx \quad (11)$$

and thermal resistance of solid region is defined as below

$$R_i = \frac{L_i}{k_i}; \quad i = 1, 2 \text{ for Solid I, Solid II} \quad (12)$$

Equations for entropy generation

Local entropy generation at each node, for thermal ($S_{h,i}$) and flow fields ($S_{f,i}$) are given by [29–32]:

$$S_{h,i} = \left[\left(\frac{\partial \theta_i}{\partial X} \right)^2 + \left(\frac{\partial \theta_i}{\partial Y} \right)^2 \right] \quad (13)$$

$$S_{f,i} = \phi \left[4 \left(\frac{\partial^2 \psi_i}{\partial X \partial Y} \right)^2 + \left(\frac{\partial^2 \psi_i}{\partial Y^2} - \frac{\partial^2 \psi_i}{\partial X^2} \right)^2 \right] \quad (14)$$

$$\phi = \frac{\mu T_h}{k} \left(\frac{\alpha}{L \Delta T} \right)^2$$

The combined total entropy generation (S_{total}) in the cavity is given by the summation of total entropy generation due to heat transfer ($S_{h,total}$) and fluid friction ($S_{f,total}$), which in turn are obtained via integrating the spatial entropy generation rates (S_h and S_f) over the domain Ω .

$$N_s = \int_{\Omega} S_h d\Omega + \int_{\Omega} S_f d\Omega = S_{h,total} + S_{f,total} \quad (15)$$

$$Be = \frac{S_{h,total}}{N_s} \quad (16)$$

where Be number present the share of thermal entropy generation.

PHYSICAL MODEL

The physical geometry considered in this study is shown in Figure 2. We consider the conjugate natural convection of a viscous incompressible fluid in a vertical enclosure in the presence of a solid with constant hot temperature T_h at the left lateral and the right lateral surface of the enclosure remains constant cold temperature (T_c). External boundaries of the upper and lower sides of enclosure are thermally insulated. It was assumed that the thermophysical properties of the material of solid and gas are temperature-independent, and the flow regime is laminar.

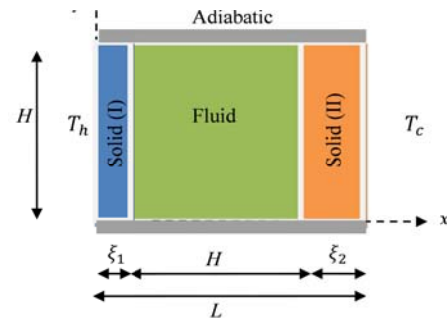


Fig. 2. Solution region of the problem

NUMERICAL PROCEDURE

The numerical simulation was done by an in-house code written in FORTRAN, using LBM. Numerical investigations were carried out for the following values of

the dimensionless parameters: $10^3 < Ra < 10^6$, $Pr=0.71$. In the numerical solution algorithm the first step is to incorporate the distribution function (DF) for both velocity and thermal field. The next steps are collision and streaming of the particles via the distribution function. Walls are placed on the sides of the computational domain. At the solid–fluid interface, in the upper, f_7, f_4, f_8 , bottom, f_6, f_2, f_5 , left f_5, f_1, f_8 and right boundary f_6, f_3, f_7 , are unknown and should be specified for streaming. Amid-grid, bounce back, no-slip boundary condition is applied to the obstacle and wall nodes to determine unknown distribution functions.

In order to use the thermal boundary condition over the solid region, regarding the difference between equilibrium DF and thermal diffusivity of the solid and fluid, the

continuity of the heat flux is required to satisfy. The comparison of streamlines, isotherms and mean Nusselt number at the interface between the solid wall and gaseous cavity with previous work at different Rayleigh numbers illustrates a fine agreement that has been obtained (Figure 3 and Table 1). As can be seen, isotherms are aligned with the temperature constant walls and slightly deviated by the flow in the cavity. This observation indicate that the heat is transferred by heat conduction in solid and the controlling heat transfer mechanism changes from conduction to convection in fluid region. Also, It should be noted that there is an excellent agreement between the present results and the benchmark solution by Varol et al. [33] (maximum difference is less than 5%).

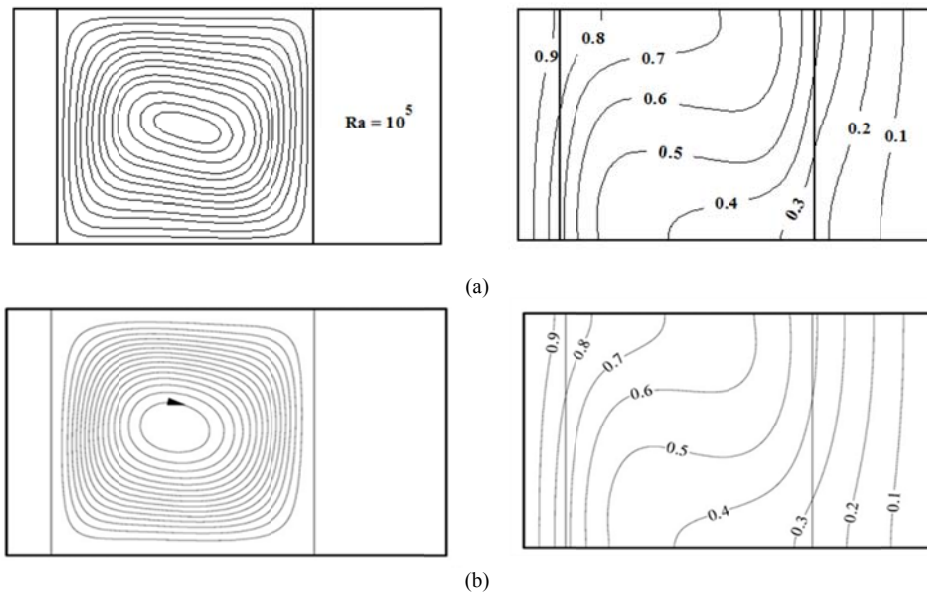


Fig. 3. Comparison the streamlines and isotherms (a) Present study (b) Varol et al. Ref. [33]

Table 1
Mean Nusselt number values for various Rayleigh numbers.

	$Ra = 10^3$		$Ra = 10^4$		$Ra = 10^5$		$Ra = 10^6$	
	$\xi_1 = \xi_2$	$0.2 L$	$0.1 L$	$0.2 L$	$0.1 L$	$0.2 L$	$0.1 L$	$0.2 L$
Present study	0.816	0.601	1.228	0.642	1.701	0.939	2.184	0.989
Varol et al. Ref. [33]	0.823	0.608	1.279	0.673	1.741	0.951	2.228	1.034

RESULTS AND DISCUSSION

A numerical study has been carried out to investigate the conjugate natural convection and entropy generation in a closed region. The effect of solid thermal resistance at $Ra = 10^4$ on the flow and thermal field are shown in Figure 4 via streamlines (on the left) and isotherm lines (on the right).

The streamlines for $Ra=10^4$ in Figure 4 reveals that one main circulations are formed.

The main circulation cell occupies region between left and right vertical wall. Isotherms are vertically distributed

on the vertical isothermal left wall while the solid bend them to the right wall. The isotherms are perpendicular to the upper and down walls due to insulated boundary condition. In addition, the isotherm labels decrease in the right solid region by increasing the R_1/R_2 ratio. This phenomenon is because of the increasing of thermal resistance in the right solid zone. Figure 5 shows Dimensionless entropy generation number and Bejan number as function of Rayleigh number at fixed thermal resistance. For lower Ra , entropy generation is mainly due

to heat transfer. Thus, Bejan number decreases and entropy generation increase by increasing Ra number. Figure 5 is given to compare results of the fixed resistance with different length (L) and thermal conductivity (k). As expected according to these results it is visible that changes

in length and thermal conductivity by keeping the resistance fixed terminate to the similar flow and thermal field. This event leads to the similar entropy generation and Bejan number.

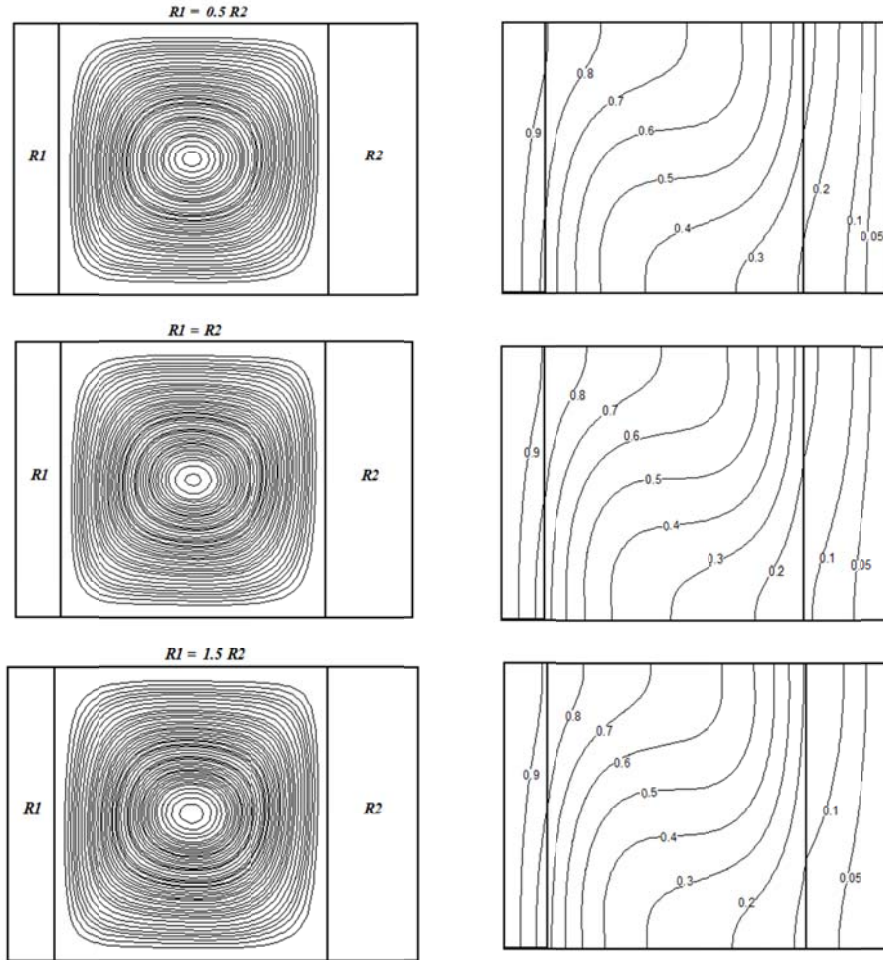


Fig. 4. Streamline for different solid thermal resistance at $Ra = 10^4$, $\xi_1 = 0.1L$, $\xi_2 = 0.2L$

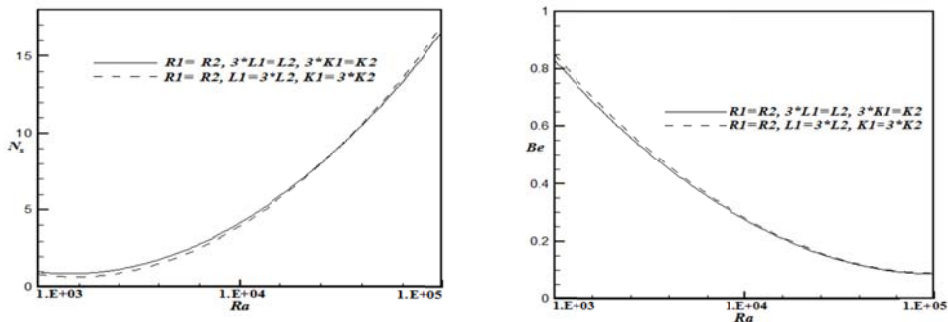


Fig. 5. Dimensionless entropy generation number and Bejan number as function of Rayleigh number at fixed thermal resistance

Figure 6 shows the Dimensionless entropy generation number as function of thermal resistance for different Rayleigh number.

Figure 6 illustrates that the entropy generation curve has an approximately minimum within the scope of $0.25 < R_1/R_2 < 1$. At this point for a detailed analysis of the phenomenon,

the averaged Nusselt number and vertical velocity magnitude were observed.

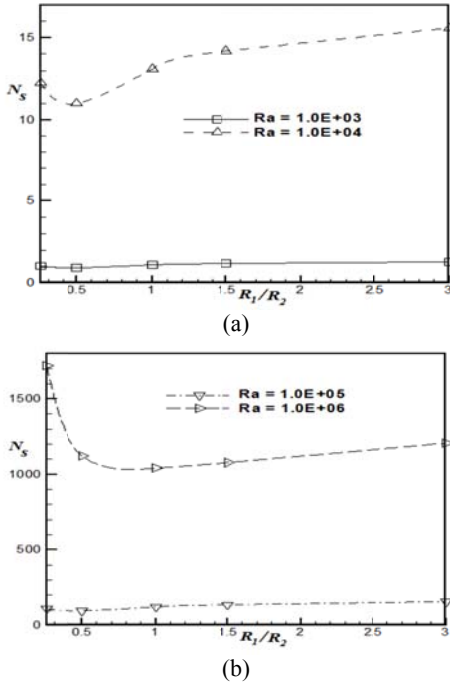


Fig. 6. Dimensionless entropy generation number as function of thermal resistance for different Ra

Table 2 and Figure 7 exhibit that the Nusselt number and the velocity have a minimum magnitude at $R_1/R_2=0.5$. These results confirm each other.

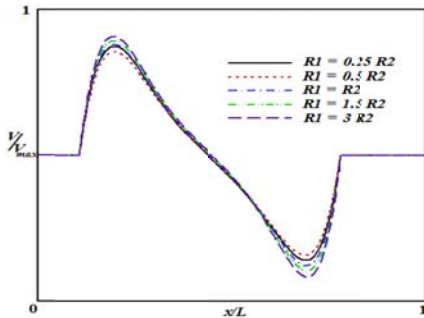


Fig. 7. Velocity profiles on the x-direction for different thermal resistance at $Ra=10^4$

Table 2

The predicted mean Nusselt number for simulating 2-D conjugate natural convection in a square cavity at $Ra=10^4$.

R_1/R_2	0.25	0.5	1	1.5	3
Over the left wall	1.258702	1.176761	1.332124	1.410923	1.513917
Over the right wall	1.168090	1.049577	1.270756	1.372554	1.496672

These consequences are consistent with the fact that by

decreasing the Nusselt number the heat flux ratio in to the fluid zone and also the velocity magnitude of fluid flow decreases and terminate to generate minimum entropy.

In this section the behavior of solid particle in a rectangular cavity due to conjugate natural convection was investigated. The fundamental theory of fluid-particle correlation has been studied by many researchers to find out the relationship of particle trajectories to the fluid paths. In this paper the approach used for the fluid particle flow is Lagrangian-Lagrangian method. Particles characteristics in the cavity can be specified by the initial particles position, the initial particles velocity and the velocity of the fluid at particle position. The fluid velocity in the system can be obtained by calculating Reynolds number of the particles with:

$$Re_p = \frac{\rho d |\bar{u} - \bar{v}_j|}{\mu} \quad (17)$$

Where Re_p is the Reynolds Number of Particle, ρ is the fluid density, d is the diameter of particle, \bar{u} is the fluid velocity, \bar{v}_j is the j^{th} particle velocity and μ is the kinematic viscosity. The mass of particle and the equation of motion for the j^{th} particle:

$$\vec{f}_{pj} = m_j \frac{d\vec{v}_j}{dt} \quad (18)$$

Figure 8 presents the flow starts from rest, with a slightly floating sphere particle placed at the top of the cavity. An initial transient movement of the particle shows before the liquid flow settles to a steady state. Locally the particle tracks align closely with the fluid streamlines. As the Rayleigh number increases, result shows the particle orbits are not smoothly distributed within the cavity. The particle trajectories agree with the paths of the passive tracers caused by the unsteady flow. This behavior results from forces pulling the macroscopic sphere towards to its preferential paths.

This result indicates that an increase in the speed can cause the particle to move slightly out of the rotation and become a passive tracer. As Rayleigh number increases from $Ra=10^3$ to 10^6 , particle paths exhibits competing trends. Moreover, spiraling trajectories unroll more and more rapidly. Particle tends to cluster more and more tightly with in a preferential orbital annulus. This annulus moves towards the periphery of the cavity.

Conclusion

Entropy generation due to conjugate laminar natural convection and particle trajectory in an enclosure is numerically predicted by using Lattice Boltzmann Method (LBM).

In comparison with conventional CFD methods, using LBM in this problem has many advantages, such as having

a simple calculation procedure, an easy to simulate complex geometries and boundary conditions. To illustrate the flexibility of the method, various parameters were investigated. In conclusion, some of the main points are briefly remarked:

I. Bejan number decreases with increasing of Rayleigh number. On the contrary, Rayleigh number enhances the heat transfer and total entropy generation rate.

II. Thermal resistance ratio has a minimum magnitude at $R_1/R_2 = 0.5$.
 III. The minimum magnitude of mean Nusselt number and velocity occur at the $R_1/R_2 = 0.5$.
 IV. As the Rayleigh number increases solid particle paths exhibit competing trends.
 V. Solid particle trajectories unroll more and more rapidly, across the lateral swaths of the flow.

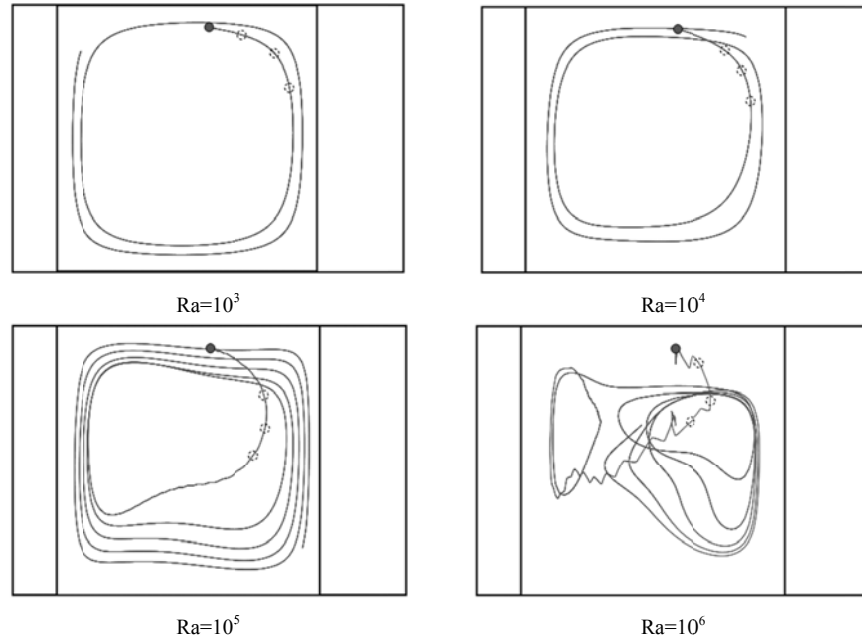


Fig. 8. Trajectory of a solid particle at different Rayleigh number

REFERENCES

- [1] J.W. Dally, P. Lall, J.C. Suhling: Mechanical Design of Electronic Systems. Knoxville, TN USA: College House Enterprises, LLS (2008).
- [2] E. Samadiani, Y. Joshi, F. Mistree: The thermal design of a next generation data center: a conceptual exposition, J. Electron 130 (2008) 1104–1112.
- [3] Y.K. Kim, K.H. Lee, H.R. Kim: Cold neutron source at KAERI, Korea, J. Nuclear Engng. and Design 238 (2008) 1664–1669.
- [4] S. Karthikeyan, T. Sundararajan, U.S.P. Shet, P. Selvaraj: Effect of turbulent natural convection on sodium pool combustion in the steam generator building of a fast breeder reactor, J. Nuclear Engng. and Design 239(2009)2992–3002.
- [5] I. Rodriguez, J. Castro, C.D. Perez-Segarra, A. Oli va: L Unsteady numerical simulation of the cooling process of vertical storage tanks under laminar natural convection, Inter. J. Thermal Sci. 48(2009)708–721.
- [6] W. Lin, S.W. Armfield: Direct simulation of natural convection cooling in a vertical circular cylinder, Int. J. Heat Mass Transfer 42 (1999) 4117–4130.
- [7] V. Kurian, M.N. Varma, A. Kannan: Numerical studies on laminar natural convection inside inclined cylinders of unity aspect ratio, Int. J. Heat Mass Transfer 52 (2009) 822–838.
- [8] G. V. Kuznetsov, M. A. Sheremet: Two-dimensional problem of natural convection in a rectangular domain with local heating and heat-conducting boundaries of finite thickness, fluid dynamics 41(2006) 881-890.
- [9] S.G. Cherkasov: Natural convection and temperature stratification in a cryogenic fuel tank in microgravity, Fluid Dynamics 29 (1994) 710–716.
- [10] V.I. Polezhaev and S.G. Cherkasov, Unsteady thermal convection in a cylindrical vessel heated from the side, Fluid Dynamics 18 (1983) 620–629.
- [11] S.G. Cherkasov: Natural convection in a vertical cylindrical vessel with heat supplied to its side and free surfaces, Fluid Dynamics 19 (1984) 902–906.
- [12] L.A. Moiseeva, S.G. Cherkasov: Mathematical modeling of natural convection in a vertical cylindrical tank with alternating-sign heat flux distribution on the wall, Fluid Dynamics 31(1996)

- 218–223.
- [13] S.G. Martyushev, M.A. Sheremet: Mathematical Modeling of the Laminar Regime of Conjugate Convective Heat Transfer in an Enclosure with an Energy Source Under Surface-Radiation Conditions,” *Journal of Engineering Physics and Thermophysics* 86 (2013) 110–119.
- [14] M.A. Sheremet: Unsteady conjugate thermo-gravitational convection in a cylindrical region with local energy source, *Thermophysics and Aeromechanics* 18 (2011) 447–458.
- [15] J. A. Esfahani, J. Alinejad: Entropy generation of conjugate natural convection in enclosures: the Lattice Boltzmann Method, *Journal of Thermophysics and Heat Transfer* 27 (2013) 498–505.
- [16] A. C. Baytas: Entropy generation for natural convection in an inclined porous cavity, *Int. J. Heat Mass Transfer* 43 (2000) 2089–2099.
- [17] G. Naterer: Transition criteria for entropy reduction of convective heat transfer from micropatterned surfaces, *J. Thermophysics and Heat Transfer* 22(2008)271-280.
- [18] A. B. S. Alquaity, S. A. Al-Dini, B. S. Yilbas: Entropy generation in microchannel flow with presence of nanosized phase change particles, *J. Thermophysics and Heat Transfer* 26(2012)134-140.
- [19] A. Vosoogh, A.R. Falahat: Effect of nanofluid on entropy generation and pumping power in coiled Tube, *J. Thermophysics and Heat Transfer* 26(2012)141-146.
- [20] S. Chakraborty, D. Chatterjee: An enthalpy-based hybrid lattice-Boltzmann method for modelling solid-liquid phase transition in the presence of convective transport , *J. Fluid Mechanics* 592 (2007) 155-176.
- [21] D. Chatterjee , S. Amiroudine : Lattice kinetic simulation of non isothermal magnetohydrodynamics, *Physical Review E* 81(2010) 1-6.
- [22] Z. Guo, T.S. Zhao: Lattice Boltzmann model for incompressible flows through porous media. *Physical Review E* 66 (2002) 304–312.
- [23] A. D’Orazio, M. Corcione, G.P Celata: Application to natural convection enclosed flows of a lattice Boltzmann BGK model coupled with a general purpose thermal boundary condition. *International Journal of Thermal Sciences* 43 (2004) 575–586.
- [24] C. Shu, Y. Peng, Y.T. Chew: Simulation of natural convection in a square cavity by Taylor series expansion and least squares-based lattice Boltzmann method. *International Journal of Modern Physics* 13 (2002) 1399–1414.
- [25] B. Chopard, P. O. Luthi: Lattice Boltzmann computations and applications to physics. *Theoret. Comput. Phys* 217 (1999) 115–130.
- [26] R. R. Nourgaliev, T. N. Dinh, T. G. Theofanous, D. Joseph: The lattice Boltzmann equation method: theoretical interpretation, numerics and implications. *Int. J. Multiph. Flow* 29 (2003) 117–169.
- [27] D. Yu, R. Mei, L. S. Luo, W. Shyy: Viscous flow computations with the method of lattice Boltzmann equation. *Progr. Aerospace. Sci* 39 (2003) 329–367.
- [28] A. A. Mohammad: Applied Lattice Boltzmann Method for Transport Phenomena Momentum Heat Mass Transfer. University of Calgary Press, Calgary (2007).
- [29] D. M. Aghajani, M. Farhadi, K. Sedighi: Effect of heater location on heat transfer and entropy generation in the cavity using the lattice Boltzmann method. *Heat Transfer Research* 40 (2009) 521–536.
- [30] A. Mezrhab, M. Jami, C. Abid, M. Bouzidi, P. Lallemand: Lattice Boltzmann modeling of natural convection in an inclined square enclosure with partitions attached to its cold wall. *Int. J. Heat Fluid Flow* 27 (2006) 456–465.
- [31] X. He, L. S. Luo: Lattice Boltzmann model for the incompressible Navier–Stokes equations. *J. Stat. Phys* 88 (1997) 927–944.
- [32] N. Thürey, U. Rüde: Stable free surface flows with the lattice Boltzmann method on adaptively coarsened grids. *Comput. Vis. Sci*12 (2009) 247–263.
- [33] Y. Varol, H. F.Oztop, A. Koca: Entropy generation due to conjugate natural convection in enclosures bounded by vertical solid walls with different thicknesses, *International Communications in Heat and Mass Transfer* 35 (2008) 648–656.